Appeared in Proc. of Post-ECCV Workshop on Biometric Authentication, LNCS 2359, pp.48-57, Denmark, June 1, 2002.

Fingerprint Matching Using Feature Space Correlation

Arun Ross[1], James Reisman[2], and Anil Jain[1]

[1] Michigan State University
East Lansing, MI, USA 48824
{rossarun, jain}@cse.msu.edu
[2] Siemens Corporate Research, Inc.
Princeton, NJ, USA 08540
james.reisman@scr.siemens.com

Abstract. We present a novel fingerprint alignment and matching scheme that utilizes ridge feature maps to represent, align and match fingerprint images. The technique described here obviates the need for extracting minutiae points or the core point to either align or match fingerprint images. The proposed scheme examines the ridge strength (in local neighborhoods of the fingerprint image) at various orientations, using a set of 8 Gabor filters, whose spatial frequencies correspond to the average inter-ridge spacing in fingerprints. A standard deviation map corresponding to the variation in local pixel intensities in each of the 8 filtered images, is generated. The standard deviation map is sampled at regular intervals in both the horizontal and vertical directions, to construct the ridge feature map. The ridge feature map provides a compact fixed-length representation for a fingerprint image. When a query print is presented to the system, the standard deviation map of the query image and the ridge feature map of the template are correlated, in order to determine the translation offsets necessary to align them. Based on the translation offsets, a matching score is generated by computing the Euclidean distance between the aligned feature maps. Feature extraction and matching takes ~ 1 second in a Pentium III, 800 MHz processor. Combining the matching score generated by the proposed technique with that obtained from a minutiae-based matcher results in an overall improvement in performance of a fingerprint matching system.

1 Introduction

The uniqueness of a fingerprint is determined by the topographic relief of its ridge structure and the presence of certain ridge anomalies termed as minutiae points (Figure 1(a)). The ridge structure in a fingerprint can be viewed as an oriented texture pattern having a *dominant* spatial frequency and orientation in a local neighborhood. The frequency is due to the inter-ridge spacing present in the fingerprint (Figure 1(b)), and the orientation is due to the flow pattern exhibited by the ridges (Figure 1(c)). By capturing the frequency and orientation of ridges in local regions in the fingerprint, a distinct representation of the fingerprint is

possible. Two such techniques of representation have been discussed in [1] and [2]. Both techniques apply a set of 8 Gabor filters to a fingerprint image; the resulting filtered images are then tessellated into cells, and the grayscale variance within a cell is used to quantify the underlying ridge structure. The grayscale variance in a cell captures the *local* ridge property, and the ordered enumeration of the tessellation captures the invariant *global* relationships among the local patterns. While in [1] a *circular* tessellation about the core point is employed, [2] uses a *square* tessellation over the entire image. Matching two fingerprints using such a representation requires a suitable alignment of the template and query images. In [1] the core point is used for alignment, while [2] uses the minutiae fields of the two fingerprint images for alignment. These techniques, however, have the following drawbacks:

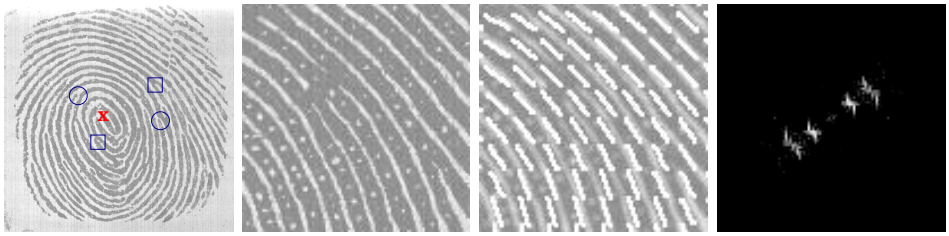

(a) (b) (c) (d)

Fig. 1. (a) A fingerprint image with the core and four minutiae points marked on it. (b) the constant inter-ridge spacing in a local region of the fingerprint; (c) the dominant direction of the ridges in (b); (d) the power spectrum of (a).

1. Detecting the core point is not an easy problem. Further, in images acquired using small solid-state sensors, the core point may not even be present, or may be present close to the boundary of the image. If the core is incorrectly detected, then the feature sets cannot be reliably compared, and in images that lack a core point, the technique described in [1] cannot be used.
2. In poor quality images (viz., images of dry fingers or fingers having cuts and bruises), the minutiae information may not be reliable due to spurious or missing minutiae points. Consequently, the alignment described in [2] may be erroneous.

To circumvent the problem of unreliable landmark points (i.e., core and minutiae points), we propose a technique that uses the extracted feature sets themselves to align and match fingerprint images. The feature set, in this case, is a ridge feature map that captures the local ridge strengths at various orientations. The local ridge characteristics are extracted via a set of Gabor filters that are pre-tuned to a specific frequency corresponding to the average inter-ridge spacing in a fingerprint image. A template fingerprint image is filtered using this set of

Gabor filters; a standard deviation map is next computed using each filtered image; the standard deviation map is then sampled at regular intervals to generate the ridge feature map. Fingerprint verification entails *correlating* the standard deviation map of the query image with the ridge feature map of the template. A two-dimensional correlation is performed thereby taking the spatial relationship between feature values into account. A matching score is generated using the Euclidean distance metric between corresponding elements in the ridge feature map of the template and the standard deviation map of the query image. Based on the matching score, and a pre-specified threshold, the query image is declared to match successfully (genuine) or unsuccessfully (impostor) with the template. In the following sections we describe the feature extraction and correlation process in more detail.

2 Ridge Feature Maps

Fingerprint matching techniques can be broadly classified as being minutiae-based or correlation-based [3]. Minutiae-based techniques attempt to align two minutiae sets to determine the total number of matched minutiae pairs [4] [5]. Correlation-based techniques, on the other hand, compare the global pattern of ridges and furrows to see if the ridge structure in the two fingerprint images align [6] [7]. The performance of minutiae-based techniques relies on the accurate detection of minutiae points and the use of sophisticated matching techniques to compare the two minutiae sets. The performance of correlation-based techniques is affected by non-linear distortions and noise present in the image. In general, it has been observed that minutiae-based techniques perform better than correlation-based ones.

Correlation-based techniques suffer from the following problems [3]: (a) A fingerprint image may have non-linear warping due to the effect of pressing a convex elastic surface (the finger) on a flat surface (the sensor). Moreover, various sub-regions in the sensed image are distorted differently due to the non-uniform pressure applied by the subject. It is difficult to compare two such distorted prints, even if translation and rotation effects are considered. (b) Based on the moisture content of the skin, the acquired images may have either thin or thick ridges. Further, the quality of the images acquired using the sensor may vary with time, thereby complicating the correlation process. Hence, an invariant[1] representation of the fingerprint is necessary if a correlation type matcher is used. As noted in the previous section, the ridge orientation in a local neighborhood of the fingerprint image has a dominant direction. Thus, features associated with the strength of the ridges (in a local neighborhood), at various orientations, may be used to represent a fingerprint image. To capture this information, $2D$ Gabor filters are used. These filters optimally capture both local orientation and frequency information very well.[2] By tuning a Gabor filter to a specific frequency

[1] Invariant to noise, distortions and ridge width variability.

[2] They are optimal in the sense that they try to minimize simultaneously the joint space-spatial frequency uncertainty [8].

and direction, the local frequency and orientation information can be obtained. An even symmetric Gabor filter has the following general form in the spatial domain:

$$G_{\theta,f}(x,y) = exp\left\{\frac{-1}{2}\left[\frac{x'^2}{\delta_x^2} + \frac{y'^2}{\delta_y^2}\right]\right\} cos(2\pi f x'), \tag{1}$$

$$x' = xsin\theta + ycos\theta,\ y' = xcos\theta - ysin\theta,$$

where f is the frequency of the sinusoidal plane wave at an angle θ with the x-axis, and δ_x and δ_y are the standard deviations of the Gaussian envelope along the x and y axes, respectively.

For extracting the response of the ridge at various orientations of the Gabor filter, the parameters (f, δ_x, δ_y, θ) are set to the following values: (i) The frequency, f, is set to correspond to the inter-ridge distance in fingerprint images. For the 300×300 (500 dpi) images obtained using the Veridicom sensor and resized to 240×240 (see section 4), the average inter-ridge spacing is about 8 pixels. Hence, $f = \frac{1}{8} = 0.125$. (ii) The selection of the standard deviation values, δ_x and δ_y, involves a trade-off. Larger values are more robust to noise, but will not capture ridge information at a fine level. Smaller values, on the other hand, are less robust to noise in the image, but capture ridge information very well. Based on empirical data [9], both these values are set to 4, i.e., $\delta_x = \delta_y = \delta = 4$. (iii) Eight different orientations are examined. These correspond to θ values of 0°, 22.5°, 45°, 67.5°, 90°, 112.5°, 135°, 157.5°. These parameters are fixed during the feature extraction process, allowing for pre-storing the Gabor filter representations in a lookup table referred to as the Gabor filter bank. This filter bank precalculates the Fourier representation of the Gabor filter for all orientations of interest. This formulation substantially improves the feature extraction time.

(a) (b) (c)

Fig. 2. (a) Original fingerprint image. (b) Fingerprint image after enhancement. (c) Fingerprint image after segmentation.

2.1 Constructing the Ridge Feature Map

The 240×240 input fingerprint image, I, is convolved with the 8 Gabor filters, $\{G_\theta\}$. Since the input image may be noisy, it is first enhanced before applying the filters. Enhancement improves the clarity of the ridge and furrow structure in the fingerprint image [10]. We use the technique described in [9] to enhance the fingerprint image (Figure 2(b)). A segmentation algorithm is also applied on the input image to identify the foreground and background regions. The foreground corresponds to those regions in the image that have ridges and furrows, while the background represents those regions that do not have this information (Figure 2(c)). Segmentation is useful during the matching phase, when the distance between two feature maps is computed.

Let H indicate the 240×240 enhanced image. Convolving H with the 8 Gabor filters in the spatial domain would be a computationally intensive operation. In order to speed-up this operation, the convolution is performed in the frequency domain. Let $\mathcal{F}(H)$ denote the discrete Fourier transform of H, and let $\mathcal{F}(G_\theta)$ indicate the discrete Fourier transform of the Gabor filter having the spatial orientation θ as described by Equation (1). Then the Gabor filtered image, V_θ, may be obtained as,

$$V_\theta = \mathcal{F}^{-1}[\mathcal{F}(H)\mathcal{F}(G_\theta)], \tag{2}$$

where $\mathcal{F}^{-1}$ is the inverse Fourier transform. 8 filtered images are obtained in this way (Figure 3). Each V_θ is used to construct a standard deviation image, S_θ, where $S_\theta(x, y)$ represents the standard deviation of the pixel intensities in a 16×16 neighborhood of (x, y) in V_θ. The standard deviation map, $S = \{S_\theta\}$, comprises of 8 images corresponding to the 8 filtered images. Thus, the standard deviation map, S, captures the variation in the ridge strength at various orientations (Figure 4). Each standard deviation image, S_θ, is then sampled at regular intervals (every 16^{th} pixel) in both the horizontal and vertical directions to obtain the ridge feature image, R_θ (Figure 5). The ridge feature map, $R = \{R_\theta\}$, is composed of these 8 images. The size of R_θ (15×15) is lesser than that of S_θ (240×240). We, therefore, have a compact fixed-length ($15 \times 15 \times 8 = 1,800$-valued) representation for the fingerprint.

3 Fingerprint Matching Using Ridge Feature Maps

The process of fingerprint matching involves comparing a query print with a set of one or more template prints. Prior to the matching process, ridge feature maps are extracted from all template images present in the database. When a query print, Q, is presented to the system, it is matched against a template ridge map, $R^T = \{R^T_\theta\}$ as follows:

1. The query image is enhanced and the set of 8 Gabor filters is applied to the enhanced image, resulting in 8 filtered images.
2. The standard deviation map, $S^Q = \{S^Q_\theta\}$, for the query image is constructed using these filtered images.

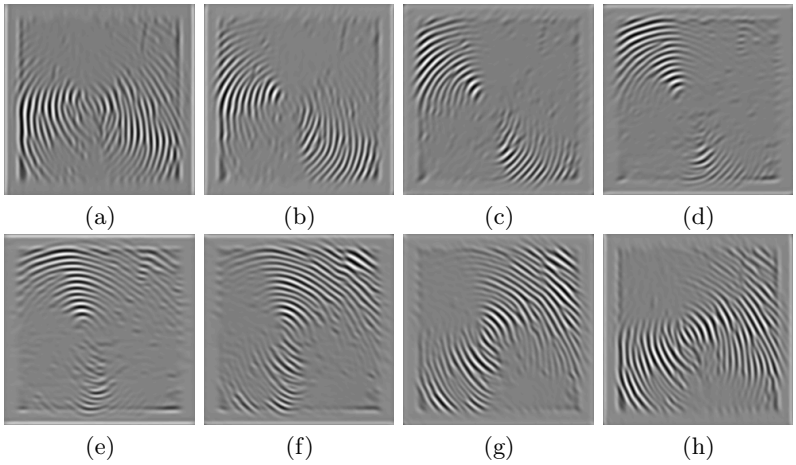

Fig. 3. Results of the filtering process on the enhanced image in Figure 2(b). The 8 images correspond to the 8 different orientations of the Gabor filter.

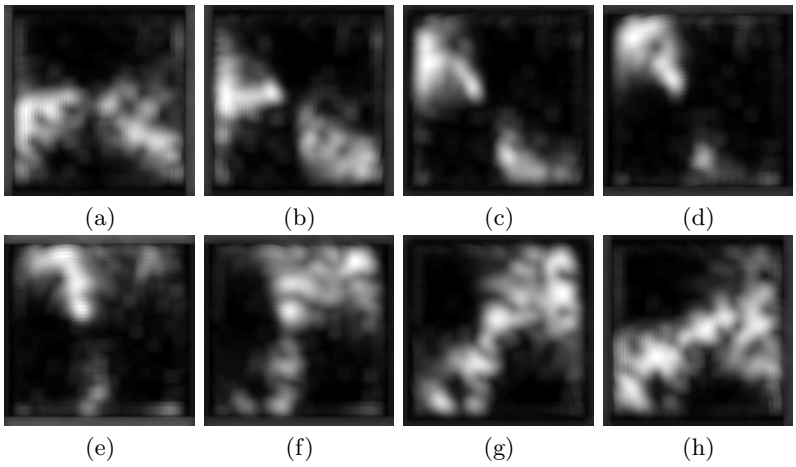

Fig. 4. The standard deviation map, $\{S_\theta\}$ of the filtered images shown in Figure 3. Each image is 240×240.

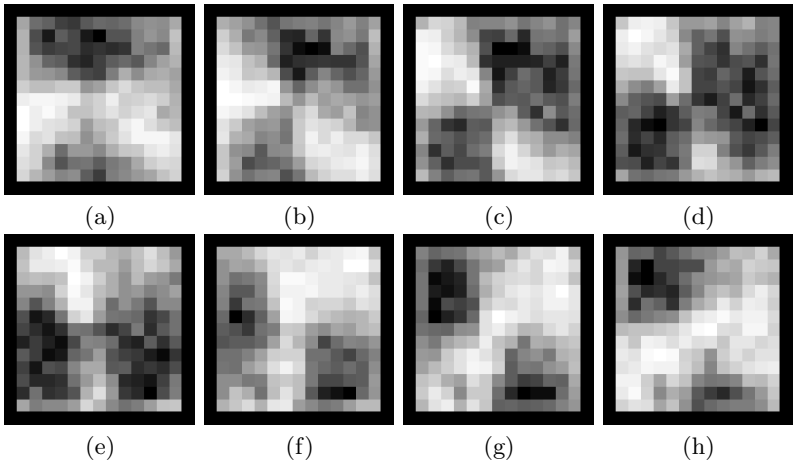

Fig. 5. The ridge feature map, $\{R_\theta\}$, of the filtered images shown in Figure 3. Each image is 15×15.

3. Each of the 8 template ridge feature images, R_θ^T, is 'expanded' to the size of S_θ^Q by interpolating with 0's. Let the ridge feature map consisting of the interpolated images be indicated by $S^T = \{S_\theta^T\}$.
4. To determine the alignment between S^Q and S^T, a $2D$ correlation of the two maps is performed. Correlation involves multiplying corresponding entries in the two maps at all possible translation offsets, and determining the sum. The offset that results in the maximum sum is chosen to be the optimal alignment between the two maps. Correlation is done in the frequency domain, and every offset is appropriately weighted. The weighting is necessary to account for the amount of overlap between the two maps. Let U_{TQ} represent the unweighted correlation matrix, and C_{TQ} represent the weighted correlation matrix. Let $N \times N$ be the size of a standard deviation image ($N = 240$). Then,

$$U_{TQ} = \sum_\theta \{\mathcal{F}^{-1}[\mathcal{F}(S_\theta^Q)\overset{*}{\mathcal{F}}(S_\theta^T)]\} \tag{3}$$

$$C_{TQ}(x,y) = \frac{U_{TQ}(x,y) * N * N}{(N-h_x)(N-w_y)}, x = 1 \ldots N, y = 1 \ldots N \tag{4}$$

where,

$$h_x = \mid [(x + \frac{N}{2}) mod N] - \frac{N}{2} \mid \text{ and } w_y = \mid [(y + \frac{N}{2}) mod N] - \frac{N}{2} \mid$$

The optimal offset (t_x, t_y) required to align S^Q with S^T is then determined as,

$$(t'_x, t'_y) = \arg\max_{x,y} \{C_{TQ}(x,y)\}, x = 1 \ldots N, y = 1 \ldots N$$

$$t_x = \begin{cases} t'_x & \text{if } t'_x < \frac{N}{2}, \\ t'_x - N & \text{if } t'_x \geq \frac{N}{2}. \end{cases} \tag{5}$$

$$t_y = \begin{cases} t'_y & \text{if } t'_y < \frac{N}{2}, \\ t'_y - N & \text{if } t'_y \geq \frac{N}{2}. \end{cases} \tag{6}$$

Equations (5) and (6) are used to decide if the offsets are negative or positive.

5. At this optimal offset, the Euclidean distance between corresponding non-zero foreground elements in $\{S_\theta^Q\}$ and $\{S_\theta^T\}$ is computed. This distance is treated as the matching score between the query print, Q and the template, T. Based on the matching score, and the pre-specified threshold, the query image is said to have matched successfully or unsuccessfully with the template.

The above procedure does not account for the rotational offset between the query and the template feature maps. To account for rotational offsets, various rotated versions of the template ridge feature map may be correlated with the query feature map, and the optimal alignment computed. Alternately, FFT-based registration techniques (like the Fourier-Mellin transform) may be employed. However this has not been implemented as yet.

4 Experiments and Results

Our database consists of fingerprint impressions (300×300) obtained from 160 users using the Veridicom sensor. Each user provided 4 different impressions (over 2 time sessions) of each of 4 different fingers - the left index finger, the left middle finger, the right index finger and the right middle finger. A set of $2,560$ ($160 \times 4 \times 4$) images were collected. The 300×300 images were resized to 240×240 (inter-ridge spacing changed from 10 pixels to 8 pixels) in order to speed-up the Fourier operations. This database is a difficult one for a fingerprint matcher due to the following reasons: (a) There is temporal variance imposed on the fingerprint impressions as they were acquired over two different time sessions. (b) The users, though cooperative, were non-habituated users of the system. (c) Some users were observed to have dry fingers that resulted in partial or faint fingerprint images. Initial experiments on this database indicate that the proposed technique provides a very good alignment of fingerprint image pairs. We compare the proposed technique with a minutiae-based matcher by plotting the Genuine Accept Rate against the False Accept Rate at various thresholds of the matching score. As expected, the minutiae-based matcher demonstrates better performance than the correlation-based matcher. However, fusing the two matchers (by normalizing and adding the matching scores) results in an improved performance of the fingerprint verification system. The ROC curves exhibiting these behaviors is shown in Figure 6.

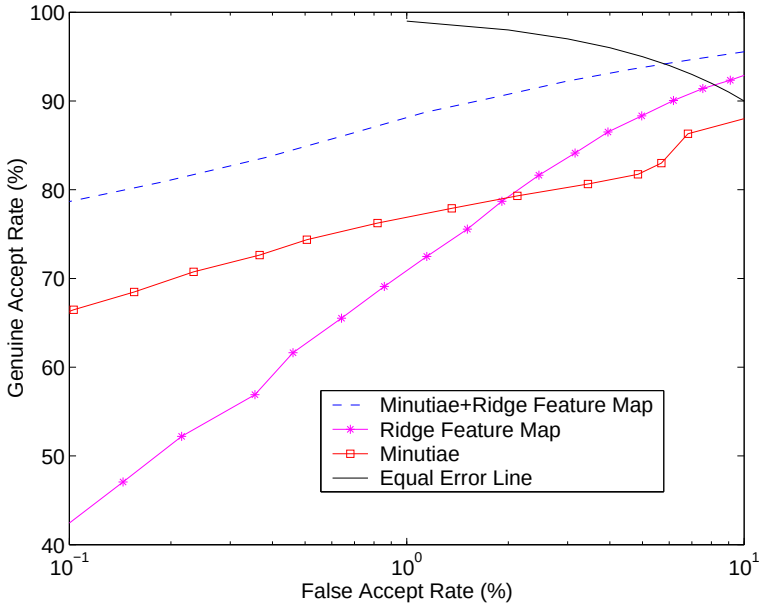

Fig. 6. ROC curves depicting matching performance.

5 Summary and Future Work

We have described a novel technique to align and match fingerprint images. The proposed technique utilizes ridge information to construct a ridge feature map that is used for representing, aligning and matching fingerprints. The ridge feature map obviates the need to use minutiae or core information to align image pairs. It also provides a compact fixed-length representation for a fingerprint image. It must be mentioned here that the performance of the proposed technique is inferior to that of a minutiae-based fingerprint matcher. However, when used alongside a minutiae matcher, an improvement in matching performance is observed. Thus, the ridge feature map complements information provided by the minutiae-based matcher. Currently we are investigating different metrics for comparing feature maps; we are also looking into ways of developing effective weighting techniques for the correlation matrix.

References

1. A. K. Jain, S. Prabhakar, L. Hong, and S. Pankanti, "Filterbank-based fingerprint matching," *IEEE Transactions on Image Processing*, vol. 9, pp. 846–859, May 2000.
2. A. K. Jain, A. Ross, and S. Prabhakar, "Fingerprint matching using minutiae and texture features," in *Proc. International Conference on Image Processing (ICIP)*, (Thessaloniki, Greece), pp. 282–285, Oct 2001.

3. L. O'Gorman, "Fingerprint verification," in *Biometrics: Personal Identification in a Networked Society* (A. K. Jain, R. Bolle, and S. Pankanti, eds.), pp. 43–64, Kluwer Academic Publishers, 1999.
4. D. Maio and D. Maltoni, "Direct gray-scale minutiae detection in fingerprints," *IEEE Transactions on PAMI*, vol. 19, pp. 27–40, Jan 1997.
5. Z. M. Kovács-Vajna, "A fingerprint verification system based on triangular matching and dynamic time warping," *IEEE Transactions on PAMI*, vol. 22, pp. 1266–1276, Nov 2000.
6. A. M. Baze, G. T. B. Verwaaijen, S. H. Gerez, L. P. J. Veelenturf, and B. J. van der Zwaag, "A correlation-based fingerprint verification system," in *Proc. ProRISC2000 Workshop on Circuits, Systems and Signal Processing*, (Veldhoven, Netherlands), Nov 2000.
7. A. Sibbald, "Method and apparatus for fingerprint characterization and recognition using auto-correlation pattern," US Patent 5633947, 1994.
8. J. Daugman, "Uncertainty relation for resolution in space, spatial frequency, and orientation optimized by two-dimensional visual cortical filters," *Journal of the Optical Society of America*, vol. 2, pp. 1160–1169, 1985.
9. L. Hong, Y. Wan, and A. K. Jain, "Fingerprint image enhancement: Algorithms and performance evaluation," *IEEE Transactions on PAMI*, vol. 20, pp. 777–789, Aug 1998.
10. D. Sherlock, D. M. Monro, and K. Millard, "Fingerprint enhancement by directional fourier filtering," *IEE Proceedings on Vision, Image and Signal Processing*, vol. 141, no. 2, pp. 87–94, 1994.